

## Magnetic Reconstruction at the (001) $\text{CaMnO}_3$ Surface

Alessio Filippetti and Warren E. Pickett

*Department of Physics, University of California at Davis, Davis, California 95616*

(Received 13 July 1999)

The Mn-terminated (001) surface of the stable antiferromagnetic insulating phase of the cubic perovskite  $\text{CaMnO}_3$  is found to undergo a magnetic reconstruction consisting of a spin-flip process at the surface: Each Mn spin at the surface flips to pair with one in the subsurface layer. In spite of very little Mn-O charge transfer at the surface, the behavior is driven by the  $e_g$  states due to the  $d_{xy} \rightarrow d_{z^2}$  charge redistribution. These results, based on local spin density theory, give a double-exchange-like coupling that is driven by the  $e_g$  character, not the additional charge, and may have relevance to colossal magnetoresistive materials.

PACS numbers: 75.30.Pd, 73.20.At, 75.25.+z, 75.30.Vn

Despite the abundance of work on manganese-based perovskites in the attempt to understand the rich panorama of their bulk properties [1,2], very little is known about their surfaces [3–5] or interfaces. The physical mechanism inducing the so-called colossal magnetoresistance (CMR) in  $\text{La}_{1-x}\text{D}_x\text{MnO}_3$  (with  $D$  a divalent alkaline earth ion, and  $x \sim 0.3$ ) is yet to be fully understood, although it seems clear that the almost half-metallic nature [2] (i.e., the complete spin polarization of the electrons at the Fermi level) plays a decisive role. The clearest evidence so far of half-metallicity is from photoemission spectra [3], whose surface sensitivity makes it essential to know the electronic structure of the surface itself. The surface introduces the likelihood of square pyramidal coordinated Mn, which is also essential to the understanding of oxygen-deficient perovskite manganites [6]. In addition, the interfacial behavior that is critical in producing low field CMR in polycrystalline material [7] and trilayer junctions [8] will involve closely related effects due to symmetry lowering of the Mn ion. Thus, studies of the surfaces of manganites are timely.

The electronic structure of the stable phase of bulk  $\text{CaMnO}_3$  has been actively investigated in recent years [2,6,9].  $\text{CaMnO}_3$  is a  $G$ -type antiferromagnetic (AFM) semiconductor. The nominal ionic picture  $\text{Ca}^{2+}\text{Mn}^{4+}\text{O}_3^{2-}$  with spherical Mn  $d^3$  configuration, makes the cubic (fcc) phase stable [10] over possible distortions observed, for instance, in  $\text{LaMnO}_3$ . In the  $G$ -type arrangement all nearest neighbors in the simple-cubic sublattice of Mn have spin-antiparallel orientation. The chemical picture of  $\text{Mn}^{4+}$  ions is represented by completely occupied  $d \uparrow_{2g}$  states. An energy gap of  $\sim 0.4$  eV separates them from the empty  $d \uparrow_g$  orbitals. Hybridization with O  $p$  states reduces the  $3\mu_B$  nominal magnetization of Mn to  $\sim 2.5 \mu_B$ , whereas magnetic moments on O or Ca are zero by symmetry.

In this paper we study the simplest manganite surface, the (001) surface of cubic  $\text{CaMnO}_3$ , to determine the surface-induced changes of structural, electronic, and magnetic properties. We find unexpectedly rich effects

of surface symmetry lowering: a spin-flip occurs on the surface Mn ions that can be traced to surface states that redistribute charge and spin among the various Mn  $d$  suborbitals and render it metallic without doping. The net effect is a short-range double-exchange-like phenomenon that relates metallicity and spin alignment, analogous to the CMR phases.

Calculations were done in a local spin density framework; the exchange-correlation potential formula by Perdew and Zunger [11] was used. A plane-wave basis with 30 Ryd cutoff energy and Vanderbilt pseudopotentials [12] make the computation viable. To establish the accuracy of our methods, which have only recently been applied to magnetic materials, in Table I we report our results for the bulk  $\text{CaMnO}_3$  in different magnetic phases. As already shown, for manganese perovskites the local spin density approximation successfully predicts the observed stable phase not only against the strongly unfavored paramagnetic (PM) phase, but also in competition with closer configurations like the ferromagnetic (FM) and the  $A$ -type AFM [made of (001) FM layers alternating along the [001] direction]. Our results are in very good agreement with those of previous all-electron linear-augmented plane-wave calculations [2]. Also, our calculated value for the equilibrium lattice constant of the  $G$ -type AFM phase (3.735 Å) is in almost perfect agreement with the experimental value (3.729 Å).

The stacking along [001] consists of alternating  $\text{MnO}_2$  and CaO units (see Fig. 1), and the surface unit cell of  $G$ -type AFM  $\text{CaMnO}_3$  is  $\sqrt{2} \times \sqrt{2}$  with respect to that of the bulk cubic cell (we neglect the very small structural distortion [10]). The (001) layers are individually AFM

TABLE I. Energies (per formula unit, referred to that of the stable  $G$ -type AFM phase) and magnetic moments on Mn atoms for the bulk  $\text{CaMnO}_3$  in different magnetic phases.

	PM	FM	$A$ AFM	$G$ AFM
$E$ (eV)	+0.56	+0.16	+0.08	0
$M$ ( $\mu_B$ )	0	2.56	2.48	2.36

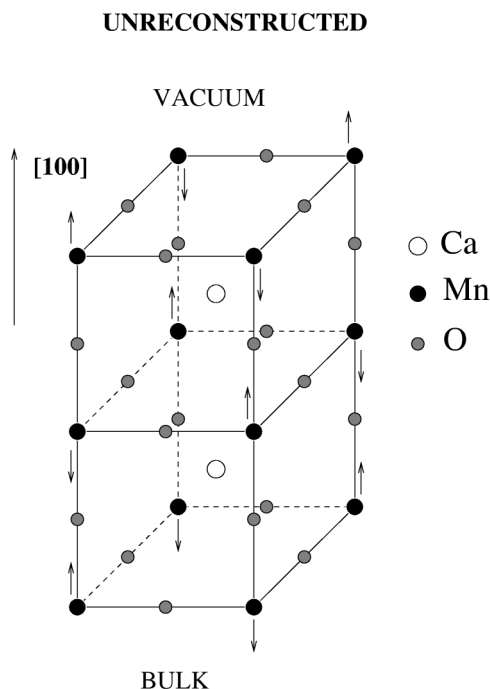


FIG. 1. Structure of the Mn-terminated (001) surface of  $G$ -type AFM  $\text{CaMnO}_3$  in the unreconstructed magnetic configuration, i.e., the spin orientation at the surface is equal to that in the bulk.

and neutral, so the surface is formally nonpolar. Surface formation produces two different surfaces, i.e., Mn terminated and Ca terminated. The presence of two inequivalent surfaces in a slab will produce fictitious fields in the vacuum that could affect the electronic and magnetic structures at the surface. We are interested in the Mn-terminated surface, since on it the effects on magnetic properties due to the surface formation are most visible. Thus we use a slab containing two identical Mn-terminated surfaces, with mirror symmetry in the central Mn layer (in total a 46-atom slab with nine layers of atoms and three of vacuum).

Surface neutrality generally favors the stability of the ideal surface against reconstructions involving strong changes of symmetry and atomic density at the surface. Therefore in this work we consider the surface with relaxed but structurally unreconstructed structure, with different types of magnetic order. Thus we will speak of “reconstruction” in a purely magnetic sense: on the unreconstructed surface the spins are oriented as in the bulk (Fig. 1), while the reconstructions involve spin-flips on the surface layer.

The structure of the two configurations that can be obtained by flipping surface spins is pictured in Fig. 2. In the left panel all surface spins are flipped, so vectors  $(\pm a, \pm a)$  remain AFM translations but each surface spin is aligned with its subsurface neighbor (spin-flip AFM: sf-AFM). In the right panel only one (of two) surface spin is flipped, leaving a FM surface layer (spin-flip FM: sf-FM).

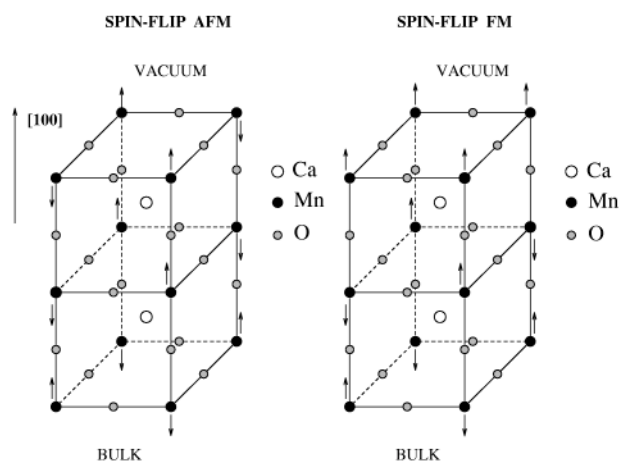


FIG. 2. Two possible magnetic reconstructions of Mn-terminated (001) surface. Left picture: spins on both Mn at the surface are flipped; the surface is still AFM. Right picture: spin on one of two Mn is flipped: FM surface.

Magnetic and relaxation energies and work functions for the three phases are reported in Table II. The  $\Delta E$ 's reported in Table II are the energies gained by relaxing all the atoms into the slab from their ideal positions. They are small and reflect the small inward atomic displacements  $\sim 1\%$  of the cubic lattice constant. This indicates a low excess stress due to the surface formation and suggests that structural reconstructions are unlikely. The work function depends very little on the spin arrangement but is largest for the most stable surface. Most significantly, the sf-AFM surface is stable against the unreconstructed one, whereas the sf-FM is the most unfavored. Thus, a quite intriguing physical picture follows: at the surface each spin prefers to pair with the one in the subsurface layer, while still keeping the AFM arrangement in plane.

It is possible to express the energy differences for differing types of magnetic order in terms of exchange constants in a Heisenberg model

$$H = - \sum_{\langle ij \rangle} J_{ij} \hat{S}_i \cdot \hat{S}_j, \quad (1)$$

where  $\hat{S}_j$  is a unit vector in the direction of the moment on site  $j$ , and the sum is over distinct pairs. For the bulk we get first and second neighbor constants  $J_1 = -26$ ,

TABLE II. Energies, per surface  $\sqrt{2} \times \sqrt{2}$  cell, of the (001)  $\text{CaMnO}_3$  surface in different magnetic phases (see the text);  $\Delta E$  (eV) are the corresponding relaxation energies, and  $W$  the work functions.

	Unrec	Spin-flip FM	Spin-flip AFM
$E$ (eV)	0	+0.12	-0.12
$\Delta E$ (eV)	0.09		0.05
$W$ (eV)	5.65	5.64	5.73

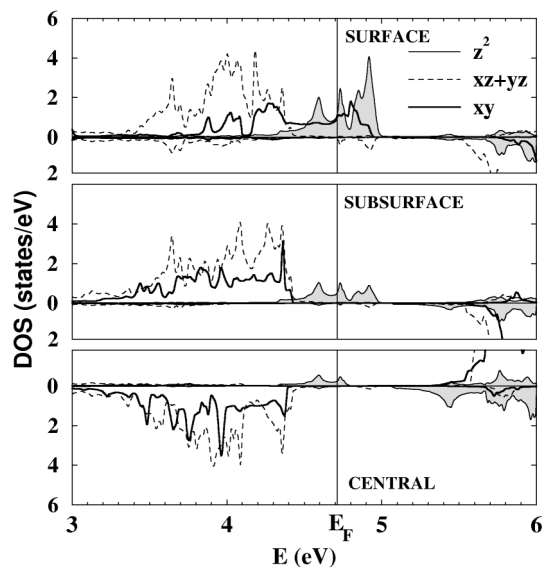


FIG. 3. Orbital-projected DOS of Mn  $d$  states for the (001) spin-flip AFM surface. Upper, middle, and lower panels refer to surface, subsurface, and central Mn atoms in the slab, respectively. Dashed, solid, and thick solid lines refer to  $d_{xz} + d_{yz}$ ,  $d_{z^2}$ , and  $d_{xy}$  orbitals, respectively. Up spin DOS is plotted upward; there is another atom in each layer whose DOS is flipped from those shown.

$J_2 = -4$  meV. This small value of  $J_2$  suggests that the nearest neighbor (nn) exchange constants contain the important contributions. From surface energies we get the nn coupling parallel and normal to the surface of  $J^{\parallel} = -22$ ,  $J^{\perp} = 29$  meV. While  $J^{\parallel}$  is close to the bulk value,  $J^{\perp}$  has the opposite sign and is larger in magnitude, indicating the FM alignment of surface and subsurface spins is robust.

The reversal of the surface-subsurface coupling can be traced to redistribution of  $d$  suborbital occupations compared to the bulk, due to the occurrence of surface states. The orbital-projected Mn  $4d$  density of states (DOS) of the stable sf-AFM phase near the Fermi level, shown in Fig. 3, makes evident the surface states that lie within the bulk band gap, which extends from  $-0.3$  to  $0.1$  eV relative to  $E_F$ . The surface states are of two distinct types,  $d_{z^2}$  and  $d_{xy}$ , reflecting the strong symmetry lowering of both  $e_g \rightarrow d_{z^2}, d_{x^2-y^2}$  and  $t_{2g} \rightarrow d_{xy}(d_{xz}, d_{yz})$  manifolds. The

surface states are almost completely polarized, a result of the large spin splitting  $\Delta_{ex} = 2$  eV that strongly inhibits hopping between ions of different spin.

Figure 4 presents the surface band structure, where for clarity, only the energy region of interest (roughly spanning the bulk gap) is shown. The  $d_{xy}$  and  $d_{z^2}$  surface states are easily identifiable. The  $d_{xy}$  states at the surface are shifted upward by 1 eV and overlap with  $d_{z^2}$  states that in the bulk hybridize strongly with the O  $p\sigma$  orbitals and form low-lying bonding and high-lying antibonding bands (most of the  $d$  weight is in the latter). The two  $d_{z^2}$  states (one from each surface of the slab) are split by 0.2 eV as a result of the interaction between Mn at opposite sides of the slab. (For a thicker slab they would converge to a single, doubly degenerate band, averaging the calculated  $d_{z^2}$  states). The  $d_{xy}$  band has a bandwidth of 1.4 eV and a dispersion that follows

$$\varepsilon_k^{xy} = -2t[\cos(k_x + k_y)a + \cos(k_x - k_y)a] \quad (2)$$

using the conventional perovskite coordinates. This dispersion arises from hopping between second nn, which are the nearest neighbors of like spin. The effective hopping amplitude is  $t = 0.17$  eV. The  $d_{z^2}$  band is very narrow (0.2 eV) and its dispersion is not easily represented by a tight binding form, reflecting small competing hopping processes along the surface (and perhaps subsurface) that are not easily identified. Coupling of the  $d_{z^2}$  state perpendicular to the surface is large, however, as reflected in the penetration of the state onto the fifth atomic layer (third Mn layer).

The net effect on the Mn ion of surface formation is an intra-atomic shift of charge from  $d_{xy}$  to the  $d_{z^2}$  orbital, without appreciable change of the charge or moment. In the solid the magnetic moment comes almost entirely from  $t_{2g}$  states, whereas on the surface  $d_{z^2}$  (surface) states contribute about 30% of the moment. Only the subsurface Mn in the sf-AFM phase experiences a net gain (0.07  $\mu_B$ ) due to the partially occupied  $d_{z^2}$  state not compensated by a depletion of  $d_{xy}$  states. In bulk, magnetic moments in the  $G$ -type bulk are allowed only on Mn, by symmetry. With the surface formation, O in plane with Ca acquire a magnetic moment as well. This is larger in the sf-AFM (0.11  $\mu_B$ ) than in the

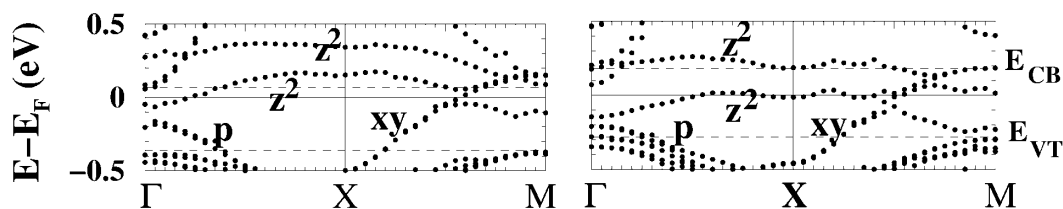


FIG. 4. Band structure in a small energy window around the Fermi energy. Left panel refers to the unreconstructed surface, right panel to the spin-flip AFM. Dashed lines are boundaries of the bulk energy gap. High symmetry points in the irreducible Brillouin zone are  $\Gamma = (0, 0, 0)$ ,  $X = (2\pi/a')(1/2, 0, 0)$ ,  $M = (2\pi/a')(1/2, 1/2, 0)$ , in the  $\sqrt{2} \times \sqrt{2}$  surface cell.

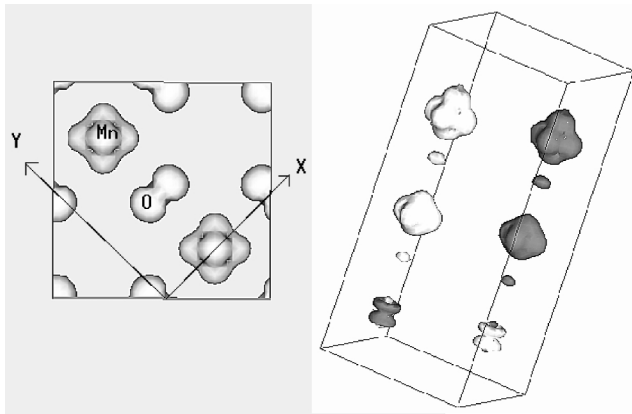


FIG. 5. Isosurface plots of the surface states for the spin-flip AFM phase. Left panel: top view of the electron charge isosurface (of  $0.01 \text{ electron/bohr}^{-3}$  magnitude) at the (100) surface. Right panel: tridimensional view of the magnetization. By inversion symmetry along  $\hat{z}$  only half the slab (five layers) is shown; on top there is the vacuum, on bottom the bulk. Light and dark isosurfaces are of the same magnitude ( $0.005 \mu_B/\text{bohr}^{-3}$ ) and opposite sign.

unreconstructed phase ( $0.06\mu_B$ ), because it is enhanced by the parallel alignment of two neighboring Mn spins.

Most of the characteristics inferred by DOS and band structure analysis can be better visualized by means of isosurface plots (Fig. 5) of charge density and magnetization of the stable sf-AFM phase. The quantities shown are due only to states within the bulk gap (see Fig. 4), thus representing charge and magnetization of the surface states. The charge density clearly shows both  $d_{xy}$  and  $d_{z^2}$  characters of the charge on Mn, as well as a  $p_{\pi}$ -type contribution from O.

The physical mechanism driving the changes in exchange interaction parameters at the surface is related to that described by Solovyev *et al.* [13] investigating how the Jahn-Teller distortions (JTD) affect the magnetic ordering of  $\text{LaMnO}_3$ . The basic driving force in the FM-to-AFM transition of  $\text{LaMnO}_3$  vs JTD is the decreasing of  $d_{z^2}$  occupancy occurring with JTD. The  $d_{z^2} - d_{z^2}$  interaction is indeed a dominant positive (i.e., FM) contribution to  $J^{\perp}$ . Also positive are the  $d_{x^2-y^2} - d_{z^2}$  and the much weaker  $d_{x^2-y^2} - d_{x^2-y^2}$  interactions, whereas  $t_{2g}$  orbitals interact by superexchange, and their contribution is AFM [13]. When the  $d_{z^2}$  orbitals are sufficiently occupied to make  $J^{\perp}$  larger than the next nearest neighbor interactions (favoring AFM) the order becomes FM along the  $\hat{z}$  axis.

In the present case the picture follows analogously: surface formation, not JTD, results in dehybridization and partial filling of the  $d_{z^2}$  states on surface (and subsurface) Mn, and a partial depletion of  $d_{xy}$  orbitals. As a consequence  $J^{\perp}$  changes sign and the magnetic ordering along  $\hat{z}$  reverses. A verification of this mechanism is given by the comparison of the band structures (or DOS) of the two competing phases (Fig. 4): in the sf-

AFM phase there is more  $d_{z^2}$  occupation and less  $d_{xy}$  depletion than in the sf-FM phase. Also, the slight occupation of  $d_{z^2}$  states on the subsurface atom is larger for the reconstructed sf-AFM phase, but not sufficient to propagate the spin alignment further into the bulk. The considerable difference with respect to the  $\text{LaMnO}_3$  JTD is that its distortion is extended, whereas at the surface the ordering is a local effect limited to the first two layers. This local spin-flip process is likely to be relevant to more general situations in manganites, such as at surfaces and interfaces of doped systems where it may affect spin transport, and at Mn sites neighboring O vacancies, as in  $\text{CaMnO}_{3-x}$  [6].

To summarize, we have described a spin-flip process at the Mn-terminated (001) surface of  $\text{CaMnO}_3$  that is driven by symmetry lowering due to surface formation which causes the partial occupation of the  $e_g d_{z^2}$  surface states. This partially occupied narrow  $d_{z^2}$  band may display correlated electron behavior. This  $d_{z^2}$  occupation reverses the magnetic alignment (from AFM to FM) at the surface in the direction orthogonal to the surface but conserves the AFM symmetry along the surface. The surface states are almost completely polarized, but AFM symmetry requires that both spin states occur in equal number, so this result may be difficult to verify experimentally.

This research was supported by the National Science Foundation Grant No. DMR-9802076. Calculations were done at the Maui High Performance Computing Center.

- 
- [1] See, for example, *Physics of Manganites*, edited by T. A. Kaplan and S.D. Mahanti (Kluwer/Plenum, New York, 1999).
  - [2] W.E. Pickett and D.J. Singh, *Phys. Rev. B* **53**, 1146 (1996).
  - [3] J.-H. Park *et al.*, *Phys. Rev. Lett.* **81**, 1953 (1998).
  - [4] J. Choi *et al.*, *Phys. Rev. B* **59**, 13453 (1999).
  - [5] H.B. Peng *et al.*, *Phys. Rev. Lett.* **82**, 362 (1999).
  - [6] G. Zampieri *et al.*, *Phys. Rev. B* **58**, 3755 (1998).
  - [7] H.Y. Hwang *et al.*, *Phys. Rev. Lett.* **77**, 2041 (1996); A. Gupta *et al.*, *Phys. Rev. B* **54**, 15629 (1996).
  - [8] Y. Lu *et al.*, *Phys. Rev. B* **54**, 8357 (1996); J.Z. Sun *et al.*, *Appl. Phys. Lett.* **70**, 1769 (1997).
  - [9] S. Satpathy *et al.*, *Phys. Rev. Lett.* **76**, 960 (1996); W.E. Pickett and D.J. Singh, *Europhys. Lett.* **32**, 759 (1995); F.F. Fava *et al.*, *J. Phys. Condens. Matter* **9**, 489 (1997).
  - [10] The very small distortion observed in some samples [Z. Zeng *et al.*, *Phys. Rev. B* **59**, 8784 (1999)] of  $\text{CaMnO}_3$  would not alter our main results.
  - [11] D.M. Ceperley and B.J. Alder, *Phys. Rev. Lett.* **45**, 566 (1980); J.P. Perdew and A. Zunger, *Phys. Rev. B* **23**, 5048 (1981).
  - [12] D. Vanderbilt, *Phys. Rev. B* **32**, 8412 (1985); K. Laasonen *et al.*, *Phys. Rev. B* **47**, 10142 (1993).
  - [13] I. Solovyev, N. Hamada, and K. Terakura, *Phys. Rev. Lett.* **76**, 4825 (1996).